A Direct and Polymer-Free Method for Transferring Graphene Grown by Chemical Vapor Deposition to Any Substrate

Wei-Hsiang Lin,[†] Ting-Hui Chen,[‡] Jan-Kai Chang,[†] Jieh-I Taur,[†] Yuan-Yen Lo,[†] Wei-Li Lee,[‡] Chia-Seng Chang,[‡] Wei-Bin Su,[‡] and Chih-I Wu[†,*]

[†]Graduate Institute of Photonics and Optoelectronics and Department of Electrical Engineering, National Taiwan University, Taipei 106, Taiwan, Republic of China, and [‡]Institute of Physics, Academia Sinica, Nankang, Taipei 11529, Taiwan, Republic of China

ABSTRACT We demonstrate a polymer-free method that can routinely transfer relatively large-area graphene to any substrate with advanced electrical properties and superior atomic and chemical structures as compared to the graphene sheets transferred with conventional polymer-assisted methods. The graphene films that are transferred with polymer-free method show high electrical conductance and excellent optical transmittance. Raman spectroscopy and X-ray/ultraviolet photoelectron spectroscopy also confirm the presence of high quality graphene sheets with little contamination after transfer. Atom-resolved images can be obtained using scanning tunneling microscope on as-transferred graphene sheets without additional cleaning process. The mobility of the polymer-free graphene monolayer is as high as 63 000 $cm^2 V^{-1} s^{-1}$, which is 50% higher than the similar sample transferred with the conventional method. More importantly, this method allows us to place graphene directly on top of devices made of soft materials, such as organic and polymeric thin films, which widens the applications of graphene in soft electronics.

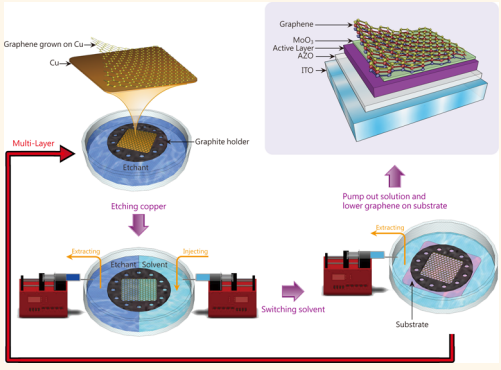

KEYWORDS: graphene · polymer-free · photoemission spectroscopy · scanning tunneling microscope · transfer

Graphene, a carbon monolayer with a two-dimensional honeycomb lattice structure, is a fascinating material due to its extraordinary electronic,[1−3] mechanical,[4] and optical properties.[5] After the first electrical measurements of monolayer graphene were published in 2004,[6] many studies were devoted to the production of isolated samples using the mechanical exfoliation of graphite. However, mechanical exfoliation[7−9] can only yield relatively small samples with noncontrollable sizes, therefore it cannot address the need for mass production of large-area and uniform monolayer graphene sheets. Other methods have also been proposed and demonstrated to produce single-layer or multiple-layer graphene; such methods include epitaxial growth on SiC,[6,10,11] oxidative/thermal intercalation and ultrasonication of graphite,[12] and recently chemical vapor deposition (CVD) on metal substrates such as nickel[13] (Ni) and copper[14] (Cu). In particular, CVD-grown graphene on Cu has drawn considerable interest due to its potential for producing high-quality large-area graphene films. These films enable various electronic applications, including touch-panel screens and organic light-emitting diodes (OLEDs).[15−17] To make microelectronic or optoelectronic devices, a reliable method is required to transfer the graphene sheets from metallic Cu substrates to various substrates, such as silicon or glass. To date, in the case of CVD-grown graphene, the common methods to transfer graphene sheets from Cu to other substrates are all involved with polymer-assisted transfer processes, in which a polymer layer such as polymethyl methacrylate (PMMA),[18−20] polydimethylsiloxane (PDMS),[21] thermal released tap,[22] poly (bisphenol A carbonate)

* Address correspondence to chihiwu@ntu.edu.tw.

Received for review December 1, 2013 and accepted January 28, 2014.

Published online January 28, 2014
10.1021/nn406170d

(PC)[23] or special self-release polymers[24] is used as a temporary rigid support to prevent folding or tearing graphene during the metal-etching step. In general, polymer-assisted transfer methods have the advantages of easy handling and processing. However, removing the residual surface contamination on the surface of graphene remains a challenge. The cleanliness of graphene is extremely important when studying its intrinsic properties, therefore removing the polymer residue after transfer is necessary and critical. Various solvent treatments and thermal annealing have been used in efforts to remove and decompose the polymer residue after the transfer process. Extensive solvent treatments and thermal annealing can remove polymer residue;[23] however, not only do these processes induce thermal stress that cause damage to the graphene without completely removing the polymer, but they also change the electronic properties and band structures of graphene. Recently, several polymer-free graphene transfer methods have been developed. For example, Regan *et al.*[25] produced 1.2 μm-diameter graphene membranes suspended on TEM grids using isopropyl alcohol to transfer between bars. However, the process using these methods can only transfer graphene in relatively small sizes, about a few tens of micrometers.

In this paper, we report a new polymer-free graphene transfer process that enables direct CVD-grown graphene to be transferred from copper to any substrate. If polymer is not used as a supporting layer, extra processes to remove polymer residues and concern about graphene surface contaminations are not needed. This polymer-free graphene transfer process can be easily repeated and enable layer-by-layer transfers of multiple stacked graphene layers. The spectrophotometer measurement shows high transmittance in the stacked graphene layers using this transfer process. In addition, the electrical properties of graphene-based transistors were measured and compared between samples produced with conventional PMMA-assisted and polymer-free transfer methods. Scanning tunneling microscopy (STM), X- ray photoelectron spectroscopy (XPS), ultraviolet photoelectron spectroscopy (UPS), and Raman spectroscopy also confirm the presence of high quality and clean graphene in this transfer process, as compared to other methods involving polymer handles.

RESULTS AND DISCISSION

The graphene films were grown on 25 μm thick poly crystalline Cu foils in a similar process reported previously.[14] In a standard polymer-based method, such as using PMMA as temporary supporting layers *via* spin-coating, a rigid support is needed for transferring graphene from Cu substrates to other substrates in order to prevent destroying the atomically thin graphene. Another interesting approach for graphene

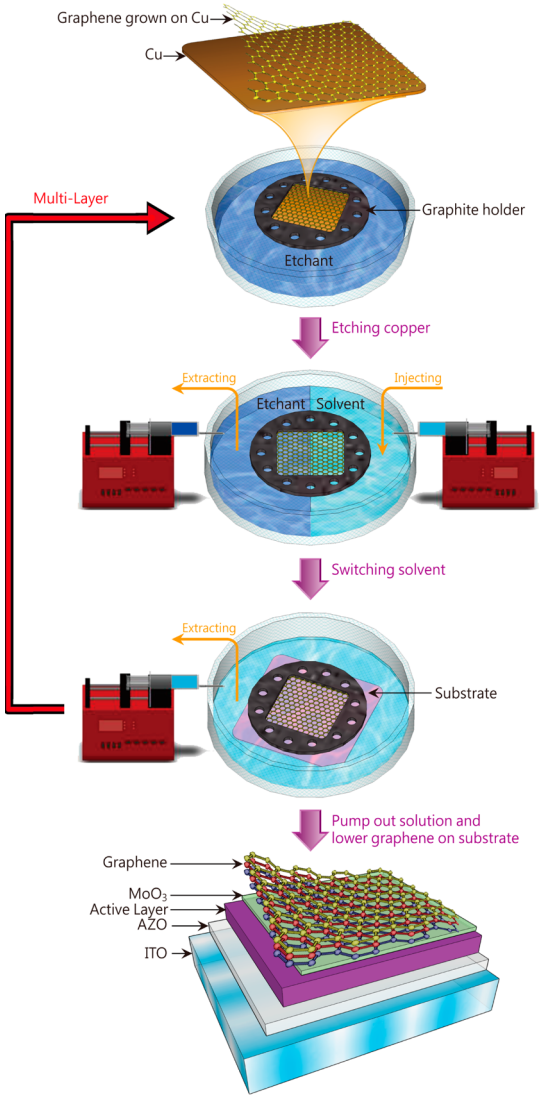

Figure 1. Schematic illustration of the polymer-free transfer process.

transfer involves using an amorphous carbon (a-C) transmission electron microscopy (TEM) grid as supporting layers.[26] To bond graphene and a-C TEM grids, a drop of isopropyl alcohol (IPA) is placed on top of the grid to wet both a-C TEM grids and underlying graphene films. As the IPA evaporates, surface tension draws graphene and a-C film into a close contact. Therefore, in our new transfer method, IPA is used to control the surface tension. The polymer-free transfer flow demonstrated in this study is shown in Figure 1. If there is no supporting material, the atomic thin graphene layer would destruct due to the surface tension of the etchant after Cu substrates are etched away. Since the surface tension of water and IPA is 72 and 21.7 dyn/cm, respectively, to control the surface tension of our etching solution, we mixed IPA and water to reduce the surface tension of the solution. To minimize the external force around graphene, we also designed a graphite holder to reduce the external force from

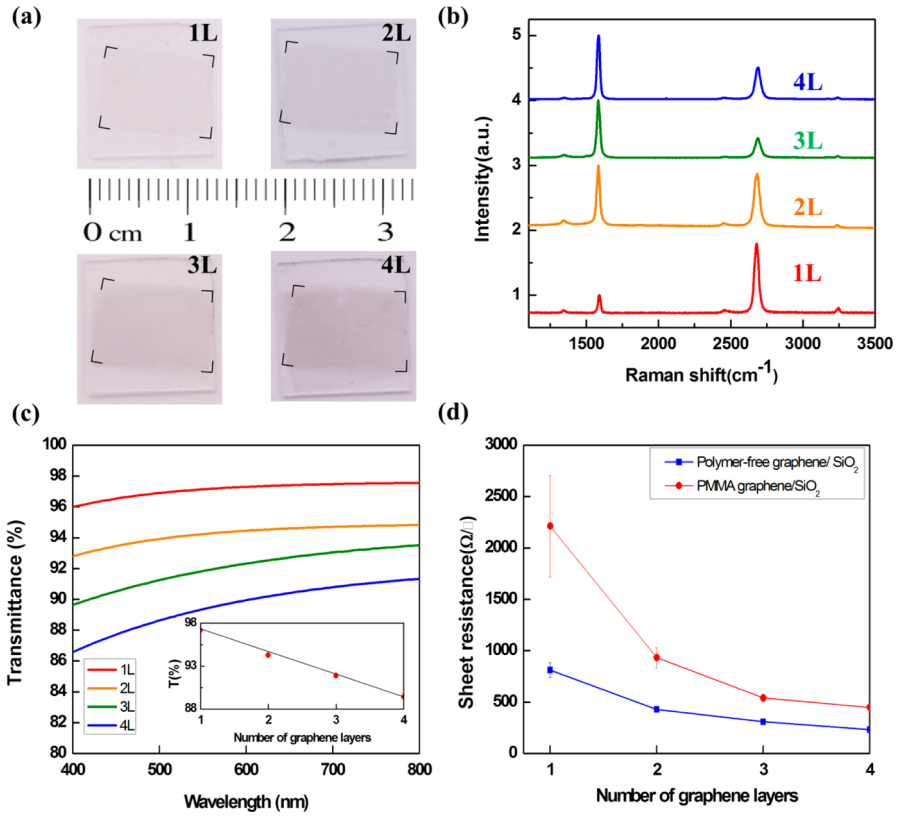

Figure 2. Optical and electrical properties of graphene sheets. (a) Photographs of 1.2 × 1.0 cm^2 films with 1−4 layers of stacked graphene film on glass. (b) Raman spectra of graphene with 1, 2, 3, and 4 layer(s). (c) Transmittance of n-layer graphene films shown in (a). The inset is the transmittance, *T*(%), at λ = 550 nm as a function of the number of stacked graphene layers, *n*. (d) The sheet resistance of graphene with different layers on SiO_2.

ambient or solution that would apply on graphene and to prevent it from degrading (folding or tearing) during the transfer process. The dimensions of the graphite holder are shown in Figure S1 of Supporting Information. All the comparisons discussed below are made between the layers from the same CVD-grown graphene sample, but being transferred with different methods.

Since graphene can be used as a transparent conductive electrode, high conductivity and optical transmittance should be not be compromised after transfer. The residual left from the conventional polymer-assisted transfer method may degrade the conductivity and transmittance of graphene sheets. Accordingly, Figure 2 shows the electrical and optical properties of graphene after transferring to glass and SiO_2 (300 nm)/Si substrates. Figure 2a shows the photographs of stacked graphene layers on the glass substrates using the polymer-free transfer process. The photograph of graphene transferred on SiO_2 substrates is in Supporting Information. The quality of transferred graphene sheets was checked with Raman spectroscopy, as shown in Figure 2b. The sharp 2D peaks at around 2700 cm^{-1} indicate that the single-layer graphene sheets are still intact with the polymer-free transfer method. As the layer number increases, the intensity of the 2D peak decreases as expected. The transmittance of the stacked graphene layers on glass substrates was measured using a spectrophotometer (Jasco, V-670). The transmittance *versus* wavelength for the stacked graphene layers is shown in Figure 2c. In addition, the inset shows the transmittance at λ = 550 nm as a function of the number of stacked graphene layers. By fitting the data to Beer's law, we find that the attenuation coefficient α is 2.65% per layer, which is near the theoretical value of 2.3%.[27,28] The slightly higher attenuation for our stacked graphene layers may result from the wrinkles induced during the transfer process. Figure 2d shows a comparison of sheet resistance between the stacked graphene layers transferred by the conventional PMMA method and the polymer-free transfer method on SiO_2 substrates. The sheet resistance of monolayer graphene and four-layer graphene transferred by the PMMA method on the SiO_2 substrate is 2.2 kΩ/□ and 450 Ω/□, respectively. On the other hand, using polymer-free transfer, the sheet resistance of monolayer graphene on SiO_2 substrates is 810 Ω/□, and that of four-layer graphene is 230 Ω/□. Although the sheet resistance will also be affected by the quality of the original graphene layers grown on Cu, we demonstrated that, from the same sample of CVD-grown graphene on Cu, the resistance of graphene sheets produced with the polymer-free transfer method is always lower than that produced with the PMMA

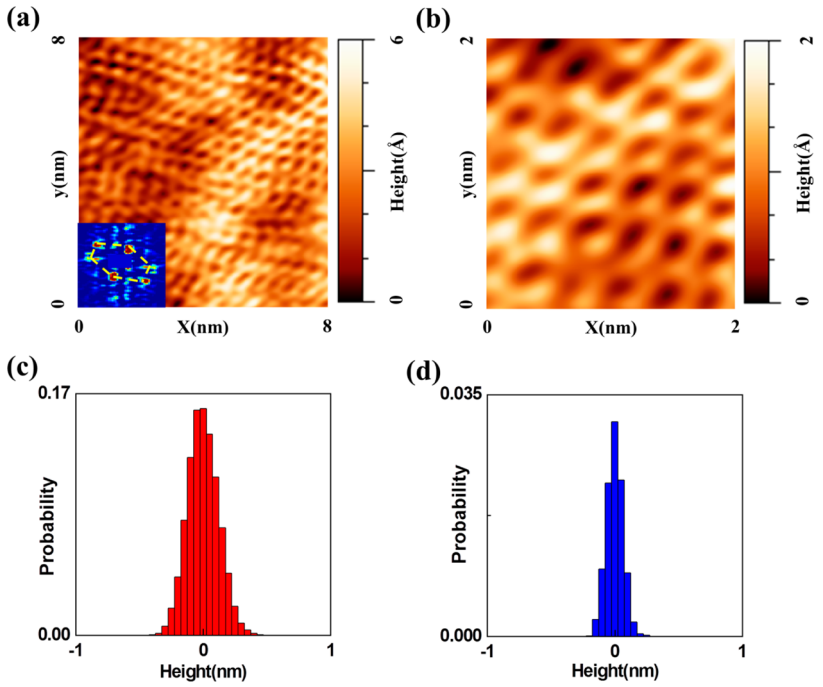

Figure 3. The representative STM image of the graphene after transfer to the Si (1 1 1) substrate, with V_{sample} = 0.2 V and I_{tunnel} = 0.1 nA. The image size is (a) 8 nm × 8 nm and (b) 2 nm × 2 nm . The inset in panel a is the Fourier transformation (FT) of large-area topography. The histogram of surface morphology of graphene is shown in panels c and d.

transfer method. The difference in the sheet resistance of graphene with these two methods may be attributed to the PMMA residues on graphene and the better surface quality of graphene transferred with the polymer-free method. To investigate these points, the chemical composition and the surface quality of graphene are studied with scanning tunneling microscopy (STM) and X-ray and ultraviolet photoemission spectroscopy (UPS and XPS).

Studies have reported atom-resolved STM images of CVD-grown graphene sheets after being transferred to other substrates. However, to retrieve STM images of graphene with atomic resolution, extra cleaning efforts need to be performed after transfer. For example, *in situ* high temperature anneal[29] is used for several hours to decompose the remaining organic residuals after the transfer processes. In our study, atom-resolved STM images of CVD-grown graphene, transferred from Cu to silicon substrate, can be obtained using polymer-free transfer method without additional *in situ* cleaning processes. Figure 3 shows representative STM images of the as-loaded graphene sheet transferred onto silicon (111) substrates. The atom-resolved honeycomb structure is clearly visible in Figure 3a with an 8 nm × 8 nm scale and also in Figure 3b with a 2 nm × 2 nm scale. As shown by the histogram in Figure 3c,d, we found the height of surface corrugations of ±0.6 nm over a lateral distance of 8 nm and ±0.3 nm over a lateral distance of 2 nm, which is in good agreement with the results reported previously.[30−32] The observed atomic spacing is consistent with the lattice constant of graphene, and the appearance of the distorted hexagonal lattice in the STM image indicates strong surface tension originating from the interaction between graphene atoms and the Si substrate.[33] STM images with atomic resolution can be achieved at many locations on the film, which indicates the excellent surface quality of the graphene sheet transferred with the polymer-free transfer method. On the other hand, for CVD-graphene transferred by the PMMA-assisted method, the atom-resolved STM images could not be obtained without using *in situ* high temperature annealing to remove PMMA residues.

In addition to atomic structures examined with STM, the chemical and electronic structures of the transferred CVD-graphene sheets are also investigated *via* UPS and XPS. Figure 4a,b shows secondary-electron onset, which represents the vacuum levels of the samples and can be used to determine its work function, and valence band spectra of polymer-free transferred graphene samples and PMMA-transferred graphene samples obtained from UPS using He II radiation. The binding energies of the spectra are all referenced to the Fermi level. The work function Φ is determined from the secondary electron energy threshold as $\Phi = h\nu - E_F - E_{cutoff}$, where $h\nu$, E_F, and E_{cutoff} are, respectively, the photon energy of He II radiation (40.8 eV), the Fermi level energy (at 0 eV since it is the reference point of the spectra), and the measured secondary-electron high-binding energy cutoff. E_{cutoff} was determined using a linear

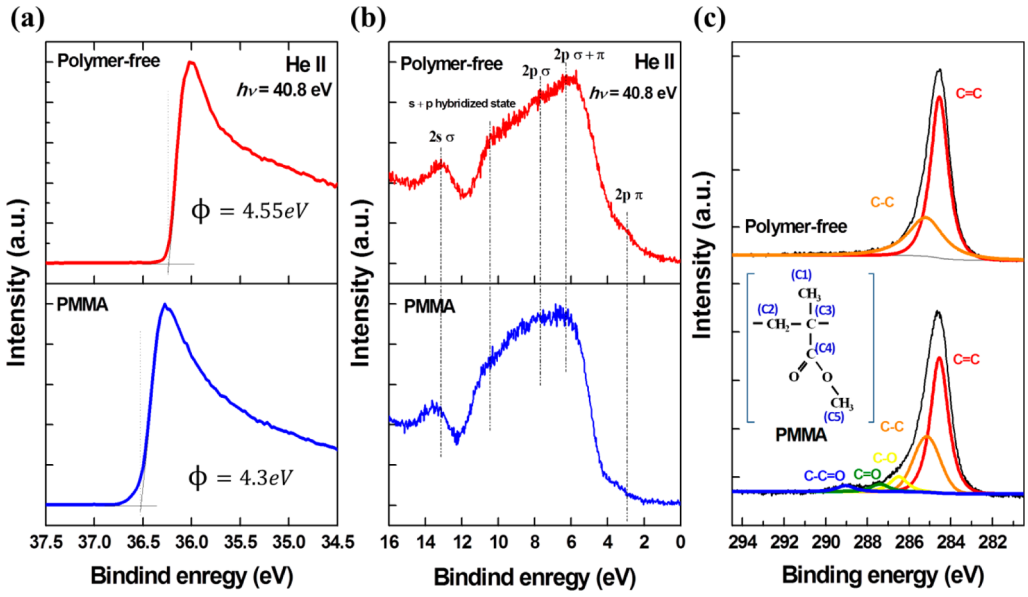

Figure 4. The ultraviolet and X-ray photoelectron spectra of graphene transferred by the polymer-free method and the PMMA method: (a) the onset of He II UPS spectra, (b) the valence-band spectra, and (c) C 1*s* core-level spectra.

extrapolation of the high binding-energy cutoff region. E_{cutoff} of the polymer-free transfer graphene film was determined to be 36.25 eV, corresponding to a work function of 4.55 eV, which is consistent with the reported value of pristine graphene film.[34] The work function of the PMMA-transferred graphene sheet is 4.3 eV. The lower work function indicates that the Fermi level is affected by the impurity left on graphene surfaces from the transfer process. Figure 4b displays the valence band spectra of the polymer-free transferred graphene. The spectra retain the main features of the pristine graphene reported previously,[35] which are C 2p π bands between 0 and 4 eV, C 2p $\sigma + \pi$ bands at roughly 6 eV, C 2p σ states at 7.9 eV, C 2s−2p hybridized states at 10.5 eV, and C 2s σ states at 13.3 eV. However, these features in the valence spectra of the PMMA-transferred graphene are relatively smeared, especially for energy levels closer to the Fermi level (*i.e.*, 2p $\sigma + \pi$ and 2p π). Parts of the delocalized 2p π states tend to bond with PMMA residues left on the graphene surface, which results in the depression of the 2p π electron states in the valence band and reduce the conductivity of the graphene sheets after being transferred.

Using XPS, chemical residues left on graphene by conventional PMMA-assisted transfer and polymer-free transfer processes are compared and examined. Figure 4c shows the carbon 1s core level spectra of graphene. In the polymer-free transferred graphene sample, the C 1s spectrum can be deconvoluted with an sp^2-hybridized C−C peak at 284.4 V (±0.1 eV) and an sp^3-hybridized C−C bond at 285.1 V (±0.1 eV), which is a result of amorphous graphitic carbon and defects.[36,37] Meanwhile, the C 1s spectrum of PMMA-transferred graphene contains various chemical bonds

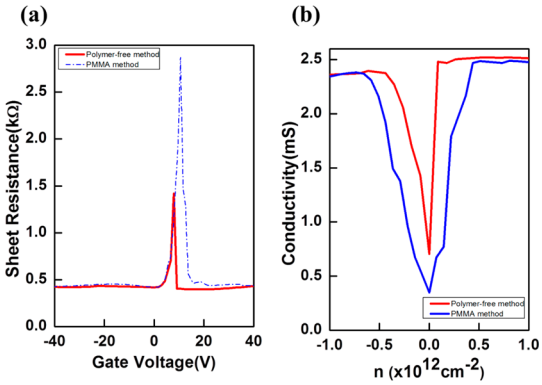

Figure 5. (a) Resistance *versus* gate voltage curves of back-gated transistors with the polymer-free graphene on BN and PMMA-transferred graphene on BN. (b) Conductivity as a function of carrier density of polymer-free graphene on BN and PMMA-assisted graphene on BN. Source-drain voltages used in these measurements are 0.3 V.

associated not only with the sp^2- and sp^3-hybridized carbon of the graphene, but also with various binding peaks from the PMMA residues on the graphene surface and extra function groups of the carbon atoms originated from PMMA (inset figure). The peaks at 286.5 eV (±0.1 eV), 287.4 eV (±0.2 eV), and 289.1 eV (±0.2 V) are associated with the bonding of carbon atoms in polymer backbone (C3), the carboxyl function group (C4), and the methoxy function group (C5) in the PMMA residues.[36,37] Both UPS and XPS data show that fully removing the PMMA residues on graphene is difficult, and the residue would affect the quality of graphene after being transferred.

Field-effect-transistors (FETs) were also fabricated with monolayer graphene sheets transferred onto boron nitride (BN)/SiO_2 (300 nm) substrates using both polymer-free and conventional methods. The BN films

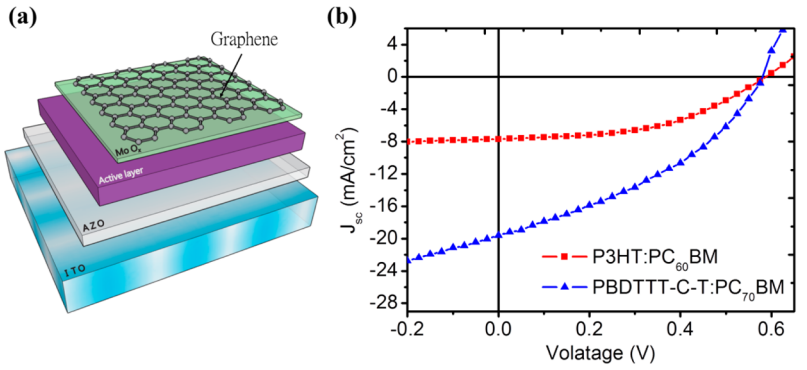

	V_{OC} (V)	J_{SC} (mA/cm^2)	FF (%)	PCE (%)
P3HT:PC_{60}BM	0.587	7.7	48.0	2.2
PBDTTT-C-T:PC_{70}BM	0.576	19.6	37.7	4.3

Figure 6. (a) The device structures of the polymer solar cells with graphene sheets as the top electrode layer. (b) The *J*−*V* characteristics of the solar cells. The device parameters are listed in the bottom.

on Cu can be purchased commercially and they were transferred to SiO_2 substrates prior to graphene transfer using the same polymer-free transfer method. The source and drain area of the back-gated FETs were defined by a shadow mask with gate lengths of 50 μm. Figure 5a shows the room-temperature electrical resistance *vs* gate voltage characteristics of FETs. The charge neutrality points of FETs with polymer-free graphene and conventional graphene monolayers are located around gate bias of 7 and 10 V, respectively. The width of the peak around the charge neutrality point for polymer-free graphene FET is much narrower than that of the conventional graphene FET, which indicates higher carrier mobility of polymer-free graphene. The field-effect mobility of the graphene-based transistor can be obtained by calculating the slop of the characteristic curve near the charge neutrality point using the Drude formula, $\mu=(1/C)d\sigma/dV$, where C denotes the capacitance of the device. The filed effect electron mobility of conventional graphene sheet on BN substrate is about 41000 $cm^2\ V^{-1}\ s^{-1}$, which is similar to the reported value of CVD-grown graphene transferred on BN substrate.[38] The mobility of polymer-free graphene monolayer on BN surface is as large as 63 000 $cm^2\ V^{-1}\ s^{-1}$, which is 50% larger than that of the graphene sheet transferred from the same CVD sample but using the conventional transfer method. Figure 5b shows the conductivity *vs* carrier concentration of the graphene-based transistor. The higher minimum conductivity of polymer-free graphene implies less structural defects in polymer-free graphene, as compared to that of the graphene sheet transferred with conventional method.[39]

This new transfer method not only can generate graphene sheets with superior properties, but also enhance capabilities in its applications to soft electronics. Most of the graphene transfer methods require pressing PMMA or other polymer templates on the targets in order to transfer graphene to other substrates, which would be difficult to place graphene sheets directly on top of the devices made of organic and polymeric materials since the mechanical force would destroy or degrade the underlying devices. As a result, in most cases graphene is used as the bottom layer in the devices, which limits the applications of graphene. Here we apply the polymer-free transfer method to make two different bulk-heterojunction polymer solar cells with graphene as the top contact layers. The device structure is illustrated in Figure 6a and the *J*−*V* (current density *versus* voltage) characteristics of the devices under AM1.5G illumination are shown in Figure 6b. The devices are so-called inverted structures with aluminum doped zinc oxide (AZO) at the bottom as cathodes and molybdenum-oxide (MoO_x)/graphene on the top as anodes. The active layers used in the solar cells are poly-3-hexylthiophene with [6.6]-phenyl-C61-butyric acid methyl-ester (P3HT:PCBM) and poly{[4,8-bis-(2-ethyl-hexyl-thiophene-5-yl)-benzo[1,2-b:4,5-*b*′]dithiophene-2,6-diyl]-*alt*-[2-(2′-ethyl-hexanoyl)-thieno[3,4-*b*]thiophen-4,6-diyl]} with [6,6]-phenyl C_{71} butyric acid methyl-ester (PBDTTT-C-T:PC_{71}BM), respectively. The power conversion efficiencies are about 2.2 and 4.3 for P3HT:PCBM and PBDTTT:PC_{70}BM based devices, even without the top reflective metals to increase the light absorption in the active layers. With the devices presented above, we show that the polymer-free transfer method not only is a superior process to transfer high quality CVD-grown graphene, but also can integrate graphene into most places of the devices, which enhances the capabilities in practical applications.

CONCLUSIONS

In summary, we demonstrated an entirely polymer-free method that can transfer large area CVD-graphene to any substrate using a graphite holder and a mixed

solution to reduce surface tensions. Compared with the conventional transfer process, the transferred CVD-graphene sheets are free of organic residues that typically remain on the surface. The polymer-free transferred graphene films also show high electrical conductance and optical transmittance that make them suitable for transparent conductive electrodes. Raman spectroscopy, scanning tunneling microscope, and X-ray (ultraviolet) photoelectron spectroscopy confirm the presence of high quality graphene with better atomic and chemical structures. Therefore, the technique presented here allows for a new means of transferring graphene onto any substrate and producing high-quality graphene sheets, which will directly expand its application on surface chemistry, biotechnology, and transparent flexible electronics.

METHODS

Polymer-Free Transfer. Figure 1 illustrates the experimental setup for the preparation of large-area monolayer graphene which can be applied on any substrate. A clean Petri dish was filled with 1:10 mixed etchant, which is made of isopropyl alcohol (IPA) and 0.1 M ammonium persulphate solution ($(NH_4)_2S_2O_8$). A thin graphite holder with a diameter of 2 cm was then carefully placed at the etchant−air boundary, serving as a confinement area for the monolayer graphene and preventing it from attaching to the edge of the holder. After copper was etched with mixed etchant, the monolayer graphene film would float on the surface of the solution. Two syringes, one empty and the other containing a mixture of DI water and IPA solution, were loaded into the syringe pump. To control the surface tension for graphene in the solution, the etchant was pumped through the transfer lines at a rate of 0.3 mL/min, and the mixed water/IPA solution was simultaneously injected at the same rate. After the etchant was totally replaced by the mixture of water and isopropyl alcohol, the substrate was placed right below the floating graphene in the solution. The solution was then pulled out with the syringe to lower the graphene onto the substrate. The sample was then heated at 60 °C in nitrogen for 10 min to dry the graphene sheets.

Characterization. The Raman spectra were taken with a WITec Alpha 300 micro-Raman imaging system. The excitation source on the sample is a 532 nm laser (2.33 eV) with a laser power below 0.1 mW to prevent laser-induced local heating. A 100× objective lens with a numerical aperture (NA) of 0.9 and a 1800 lines/mm grating was used in the Raman measurement. Photoemission spectra were measured with PHI 5400 system from Perkin-Elmer with Mg and Al as the X-ray anodes and He discharge lamp as the ultraviolet photon sources. Scanning tunneling microscopy was carried out with an Omicron system at room temperature.

Conflict of Interest: The authors declare no competing financial interest.

Acknowledgment. The authors would like to thank W. Y. Chan and F. C. Chien for their help in Raman spectroscopy measurements. This work is supported by National Science Council of the Republic of China (NSC 101-2628-M-002-004-MY3) and the Center for Emerging Materials and Advanced Devices, National Taiwan University.

Supporting Information Available: Additional experimental details. This material is available free of charge *via* the Internet at http://pubs.acs.org.

REFERENCES AND NOTES

1. Castro Neto, A. H.; Guinea, F.; Peres, N. M. R.; Novoselov, K. S.; Geim, A. K. The Electronic Properties of Graphene. *Rev. Mod. Phys.* **2009**, *81*, 109–162.
2. Novoselov, K. S.; Geim, A. K.; Morozov, S. V.; Jiang, D.; Katsnelson, M. I.; Grigorieva, I. V.; Dubonos, S. V.; Firsov, A. A. Two-Dimensional Gas of Massless Dirac Fermions in Graphene. *Nature* **2005**, *438*, 197–200.
3. Geim, A. K.; Novoselov, K. S. The Rise of Graphene. *Nat. Mater.* **2007**, *6*, 183–191.
4. Lee, C.; Wei, X.; Kysar, J. W.; Hone, J. Measurement of the Elastic Properties and Intrinsic Strength of Monolayer Graphene. *Science* **2008**, *321*, 385–388.
5. Nair, R. R.; Blake, P.; Grigorenko, A. N.; Novoselov, K. S.; Booth, T. J.; Stauber, T.; Peres, N. M. R.; Geim, A. K. Fine Structure Constant Defines Visual Transparency of Graphene. *Science* **2008**, *320*, 1308.
6. Berger, C.; Song, Z. M.; Li, T. B.; Li, X. B.; Ogbazghi, A. Y.; Feng, R.; Dai, Z. T.; Marchenkov, A. N.; Conrad, E. H.; First, P. N.; *et al.* Ultrathin Epitaxial Graphite: 2D Electron Gas Properties and a Route toward Graphene-Based Nanoelectronics. *J. Phys. Chem. B* **2004**, *108*, 19912–19916.
7. Lu, X. K.; Yu, M. F.; Huang, H.; Ruoff, R. S. Tailoring Graphite with the Goal of Achieving Single Sheets. *Nanotechnology* **1999**, *10*, 269–272.
8. Lu, X. K.; Huang, H.; Nemchuk, N.; Ruoff, R. S. Patterning of Highly Oriented Pyrolytic Graphite by Oxygen Plasma Etching. *Appl. Phys. Lett.* **1999**, *75*, 193–195.
9. Novoselov, K. S.; Geim, A. K.; Morozov, S. V.; Jiang, D.; Zhang, Y.; Dubonos, S. V.; Grigorieva, I. V.; Firsov, A. A. Electric Field Effect in Atomically Thin Carbon Films. *Science* **2004**, *306*, 666–669.
10. Rollings, E.; Hussain, B. S.; Gweon, G.-H.; Zhou, S. Y.; Mun, B. S.; Fedorov, A. V.; Lanzara, A. Synthesis and Characterization of Atomically Thin Graphite Films on a Silicon Carbide Substrate. *J. Phys. Chem. Solids* **2006**, *67*, 2172–2177.
11. Unarunotai, S.; Koepke, J. C.; Tsai, C.-L.; Du, F.; Chialvo, C. E.; Murata, Y.; Haasch, R.; Petrov, I.; Mason, N.; Shim, M.; Lyding, J.; Rogers, J. A. Layer-by-Layer Transfer of Multiple, Large Area Sheets of Graphene Grown in Multilayer Stacks on a Single SiC Wafer. *ACS Nano* **2010**, *4*, 5591–5598.
12. McAllister, M. J.; Li, J.-L.; Adamson, D. H.; Schniepp, H. C.; Abdala, A. A.; Liu, J.; Herrera-Alonso, M.; Milius, D. L.; Car, R.; Prud'homme, R. K.; *et al.* Single Sheet Functionalized Graphene by Oxidation and Thermal Expansion of Graphite. *Chem. Mater.* **2007**, *19*, 4396–4404.
13. Reina, A.; Jia, X.; Ho, J.; Nezich, D.; Son, H.; Bulovic, V.; Dresselhaus, M. S.; Kong, J. Large Area, Few-Layer Graphene Films on Arbitrary Substrates by Chemical Vapor Deposition. *Nano Lett.* **2009**, *9*, 30–35.
14. Li, X.; Cai, W.; An, J.; Kim, S.; Nah, J.; Yang, D.; Piner, R.; Velamakanni, A.; Jung, I.; Tutuc, E.; *et al.* Large-Area Synthesis of High-Quality and Uniform Graphene Films on Copper Foils. *Science* **2009**, *324*, 1312–1314.
15. Bonaccorso, F.; Sun, Z.; Hasan, T.; Ferrari, A. C. Graphene photonics and optoelectronics. *Nat. Photonics* **2010**, *4*, 611–622.
16. Pang, S.; Hernandez, Y.; Feng, X.; Müllen, K. Graphene as Transparent Electrode Material for Organic Electronics. *Adv. Mater.* **2011**, *23*, 2779–2795.
17. Phaedon, A. Graphene: Electronic and Photonic Properties and Devices. *Nano Lett.* **2010**, *10*, 4285–4294.
18. Li, X.; Zhu, Y.; Cai, W.; Borysiak, M.; Han, B.; Chen, D.; Piner, R. D.; Colombo, L.; Ruoff, R. S. Transfer of Large-Area Graphene Films for High-Performance Transparent Conductive Electrodes. *Nano Lett.* **2009**, *9*, 4359–4363.
19. Suk, J. W.; Kitt, A.; Magnuson, C. W.; Hao, Y.; Ahmed, S.; An, J.; Swan, A. K.; Goldberg, B. B.; Ruoff, R. S. Transfer of CVD-Grown Monolayer Graphene onto Arbitrary Substrates. *ACS Nano* **2011**, *5*, 6916–6924.

20. Alfonso, R.; Hyungbin, S.; Liying, J.; Ben, F.; Dresselhaus, M. S.; Liu, Z.; Kong, J. Transferring and Identification of Single- and Few-Layer Graphene on Arbitrary Substrates. *J. Phys. Chem. C* **2008**, *112*, 17741–17744.
21. Kim, K. S.; Zhao, Y.; Jang, H.; Lee, S. Y.; Kim, J. M.; Kim, K. S.; Ahn, J.-H.; Kim, P.; Choi, J.-Y.; Hong, B. H. Large-Scale Pattern Growth of Graphene Films for Stretchable Transparent Electrodes. *Nature* **2009**, *457*, 706–710.
22. Bae, S.; Kim, H.; Lee, Y.; Xu, X.; Park, J. S.; Zheng, Y.; Balakrishnan, J.; Lei, T.; Kim, H. R.; Song, Y. I.; *et al.* Roll-to-Roll production of 30-in. graphene films for transparent electrodes. *Nat. Nanotechnol.* **2010**, *5*, 574–578.
23. Lin, Y.-C.; Jin, C.; Lee, J.-C.; Jen, S.-F.; Suenaga, K.; Chiu, P.-W. Clean Transfer of Graphene for Isolation and Suspension. *ACS Nano* **2011**, *5*, 2362–2368.
24. Song, J.; Ksm, F.-Y.; Png, R.-Q.; Seah, W.-L.; Zhuo, J.-M.; Lim, G.-K.; Ho, P. K. H.; Chua, L.-L. A General Method for Transferring Graphene onto Soft Surfaces. *Nat. Nanotechnol.* **2013**, *8*, 356–362.
25. Regan, W.; Alem, N.; Alemán, B.; Geng, B.; Girit, Ç.; Maserati, L.; Wang, F.; Crommie, M.; Zettl, A. A Direct Transfer of Layer-Area Graphene. *Appl. Phys. Lett.* **2010**, *96*, 113102.
26. Ledwosinska, E.; Gaskell, P.; Guermoune, A.; Siaj, M.; Szkopek, T. Organic-Free Suspension of Large-Area Graphene. *Appl. Phys. Lett.* **2012**, *101*, 033104.
27. Nair, R. R.; Blake, P.; Grigorenko, A. N.; Novoselov, K. S.; Booth, T. J.; Stauber, T.; Peres, N. M. R.; Geim, A. K. Fine Structure Constant Defines Visual Transparency of Graphene. *Science* **2009**, *324*, 1312–1314.
28. Blake, P.; Brimicombe, P. D.; Nair, R. R.; Booth, T. J.; Jiang, D.; Schedin, F.; Ponomarenko, L. A.; Morozov, S. V.; Gleeson, H. F.; Hill, E. W.; *et al.* Graphene-Based Liquid Crystal Device. *Nano Lett.* **2008**, *8*, 1704–1708.
29. Ishigami, M.; Chen, J. H.; Cullen, W. G.; Fuhrer, M. S.; Williams, E. D. Atomic Structure of Graphene on SiO_2. *Nano Lett.* **2007**, *7*, 1643–1648.
30. Stolyarova, E.; Taeg Rim, K.; Ryu, S.; Maultzsch, J.; Kim, P.; Brus, L. E.; Heinz, T. F.; Hybertsen, M. S.; Flynn, G. W. High-Resolution Scanning Tunneling Microscopy Imaging of Mesoscopic Graphene Sheets on an Insulating Surface. *Proc. Natl. Acad. Sci. U.S.A.* **2007**, *104*, 9209–9212.
31. Cortijoa, A.; Vozmediano, M. A. H. Effects of Topological Defects and Local Curvature on the Electronic Properties of Planar Graphene. *Nucl. Phys. B* **2007**, *763*, 293–308.
32. Meyer, J. C.; Geim, A. K.; Katsnelson, M. I.; Novoselov, K. S.; Booth, T. J.; Roth, S. The Structure of Suspended Graphene Sheets. *Nature* **2007**, *446*, 60–63.
33. Ishigami, M.; Chen, J. H.; Cullen, W. G.; Fuhrer, M. S.; Williams, E. D. Atomic Structure of Graphene on SiO_2. *Nano Lett.* **2007**, *7*, 1643–1648.
34. Yu, Y.-J.; Zhao, Y.; Ryu, S.; Brus, L. E.; Kim, K. S.; Kim, P. Tuning the Graphene Work Function by Electric Field Effect. *Nano Lett.* **2009**, *9*, 3430–3434.
35. Luo, Z.; Shang, J.; Lim, S.; Li, D.; Xiong, Q.; Shen, Z.; Lin, J.; Yu, T. Modulating the Electronic Structures of Graphene by Controllable Hydrogenation. *Appl. Phys. Lett.* **2010**, *97*, 233111.
36. Hong, S. K.; Song, S. M.; Sul, O.; Cho, B. J. Carboxylic Group as the Origin of Electrical Performance Degradation during the Transfer Process of CVD Growth Graphene. *J. Electrochem. Soc.* **2012**, *159*, K107–K109.
37. Pirkle, A.; Chan, J.; Venugopal, A.; Hinojos, D.; Magnuson, C. W.; McDonnell, S.; Colombo, L.; Vogel, E. M.; Ruoff, R. S.; Wallace, R. M. The Effect of Chemical Residues on the Physical and Electrical Properties of Chemical Vapor Deposited Graphene Transferred to SiO_2. *Appl. Phys. Lett.* **2011**, *99*, 122108.
38. Gannett, W.; Regan, W.; Watanabe, K.; Taniguchi, T.; Crommie, M. F.; Zettl, A. Boron Nitride Substrates for High Mobility Chemical Vapor Deposited Graphene. *Appl. Phys. Lett.* **2011**, *98*, 242105.
39. Hwang, E. H.; Adam, S.; Das Sarma, S. Carrier Transport in Two-Dimensional Graphene Layers. *Phys. Rev. Lett.* **2007**, *98*, 186806.